AIRBORNE RADIOACTIVITY PRODUCED AT ELECTRON ACCELERATORS COMPARISON BETWEEN MEASUREMENT AND THEORY

P. Jost, H.-P. Weise
Bundesanstalt für Materialprüfung (BAM)
Berlin

1.) Introduction

In the atmosphere around low energy (< 100 MeV) electron accelerators two radionuclides of concern are ^{13}N and ^{15}O which are produced by (γ,n) reactions from ^{14}N and ^{16}O. The half lives of these positron-emitters are 10 min and 2,03 min respectively. In order to obtain reliable data for estimating the radiation exposure caused by gaseous radionuclides within the accelerator installation and in the environment, the concentrations of the radioactive gases were measured on the axis of the primary X-ray beam and at various points in the accelerator room. These measurements were performed at a 35 MeV electron linear accelerator and a 45 MeV betatron.

As a detector for gaseous ß-emitters a conventional device consisting of a 70 l steel barrel with two large GM tubes inside (one of them shielded against ß-radiation) and a differential counter for background compensation was used. The radioactive gas produced in a small irradiation chamber on the axis of the X-ray beam was pumped into the measuring barrel located in a separate well shielded room. The concentration in the accellerator room outside the collimated X-ray beam was determined by directly (without an irradiation chamber) pumping the activated air into the measuring device. The contributions of ^{13}N and ^{15}O to the total gas activity were evaluated by decomposition of decay curves. The experimental values of the activity concentrations on the X-ray beam axis were compared with the effective cross sections of the reactions $^{14}N(\gamma,n)^{13}N$ and $^{16}O(\gamma,n)^{15}O$. Good agreement between measurement and theory was obtained.

2.) In Beam Concentration of Radioactivity

The saturated concentration of radioactivity C_{A_s} in forward direction at distance r from target is given by:

$$C_{A_s} = n \cdot \sigma_{eff} \cdot C_{eff} \cdot \dot{J}(r_0,o^0) \cdot \frac{r_0^2}{r^2} \qquad (1)$$

$$\sigma_{eff} = \int_0^{E_0} \sigma(E) f(E,E_0)\,dE \text{ mit } \int_0^{E_0} f(E,E_0)\,dE = 1 \qquad (2)$$

$$C_{eff} = \left[\int_0^{E_0} \frac{f(E,E_0)}{C(E)}\,dE \right]^{-1} \qquad (3)$$

n — number of atoms of the parent target element (^{14}N resp. ^{15}O) in 1 cm^3 of atmospheric air

σ_{eff} — effective cross section (fig. 4)

C_{eff} — effective conversion factor between exposure rate and flux density (fig.5)

$\dot{J}(r_0,o^0)$ — exposure in forward direction ($\Theta_0 = o^0$) at reference distance r_0 (fig. 6)

$f(E,E_0)$ — normalized X-ray spectrum in forward direction (fig. 3)

The activity concentrations C_{A_s} per unit exposure rate at electron energy E_0= 30 MeV are given in Table I.

3. Activity Concentration outside Beam

The activity concentration in the accelerator room depends on the total activity in the irradiated air volume and the distribution of the radioactive gas in the target room by diffusion and convection. Assuming that photons are emitted within a narrow cone of opening α around 0^0 and of length R the total activity is evaluated by integration of equation (1):

$$A_{S\ tot} = n \cdot \sigma_{eff} \cdot C_{eff} \cdot \dot{J}(r_0,0^0) \cdot r_0^2 \cdot 2\pi R \cdot (1 - \cos\alpha) \qquad (4)$$

For a broad X-ray beam the angular distribution $g(\Theta)$ of the photons must be considered:

$$A_{S\ tot} = n \cdot \sigma_{eff} \cdot C_{eff} \cdot \dot{J}(r_0,0^0) \cdot r_0^2 \cdot 2\pi R \cdot \int_0^{\alpha} g(\Theta)\sin\Theta d\Theta \qquad (5)$$

$$g(\Theta=0^0) = 1$$

In equation (5) the dependence of the bremsstrahlung spectrum from angel (Θ) of emergence has not been regarded. This is a conservative estimation, because the closer the angle of emergence is to 0^0, the harder is the spectrum. Assuming a homogeneous distribution of the total activity produced within the X-ray cone over the accelerator room with volume V_R yields the off-axis concentration:

$$\bar{C}_{A_S} = A_{S\ tot}/V_R \qquad (6)$$

4.) Results

In Table I. the experimental and calculated values are listed. The parameters are: E = 30 MeV, $\alpha = 4^0$, R= 350 cm, $V_R = 500\ m^3$

Table I. Saturation Activity per Exposure Rate $\dot{J}(r_0,0^0)$ $[Ci \cdot m^{-3} \cdot R^{-1} \cdot min]$

^{13}N	^{15}O		
$2,7 \cdot 10^{-6}$	$0,88 \cdot 10^{-6}$	experimental	on beam axis
$1,8 \cdot 10^{-6}$	$1,1 \cdot 10^{-6}$	calculated	
$6,2 \cdot 10^{-11}$	$2,5 \cdot 10^{-11}$	experimental	in centre of target room
$6,0 \cdot 10^{-11}$	$3,8 \cdot 10^{-11}$	calculated	

By comparison of the experimental and theoretical values the following conclusions can be drawn:

1. The activity concentration in the X-ray beam can be calculated with sufficient accuracy by folding the cross section with the normalized bremsstrahlung spectrum.

2. Assuming perfect mixing of the air the activity concentration in the room can be estimated by the ratio between the total activity produced within the X-ray cone and the room volume.

3. If there is no homogeneous distribution of the gaseous activity in the accelerator room, the assumption of a homogenous distribution yields a conservative estimation of the off-axis concentration and hence an overestimation of the dose equivalent as well to the public by exhaust radioactive gas as to the staff entering the target room after shut down of the accelerator.

5.) Dose Equivalent for Submersion

With the dosimetric data in ICRP Publication 30 dose factors for occupational exposure by submersion in a cloud of gas are derived. The dose factors are listed in Table II as a function of the volume of the radioactive cloud.

Table II Dose Factors $[rem \cdot h^{-1} \cdot Ci^{-1} \cdot m^3]$ for Different Volumes of Radioactive Cloud

Volume		∞/2	1000 m^3	500 m^3	100 m^3
^{13}N	γ-Subm.	590	27	22	13
	β-Subm.	370	370	370	370
^{15}O	γ-Subm.	590	28	23	14
	β-Subm.	630	630	630	630

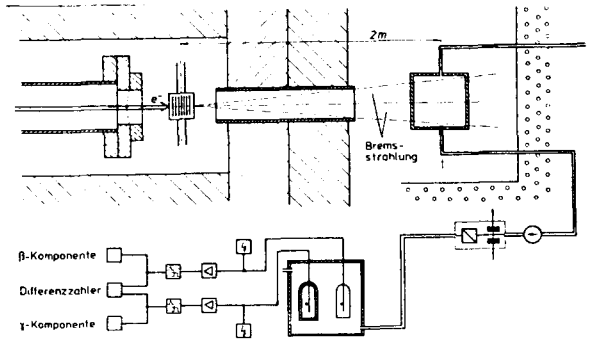

Fig. 1 Experimental set-up for in beam measurement of the activity concentration

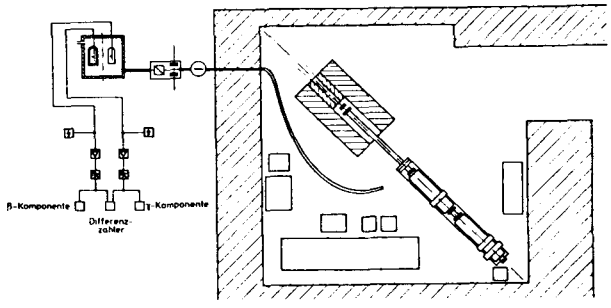

Fig. 2 Experimental set-up for measurement of the activity concentration at different locations in the target room

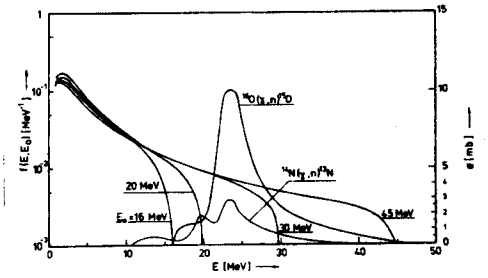

Fig. 3 Normalized Bremsstrahlung spectra and cross sections for (γ,n)-reactions

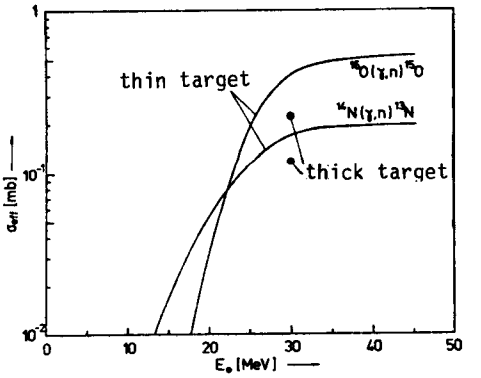

Fig. 4 Effective cross sections for (γ,n)-reactions

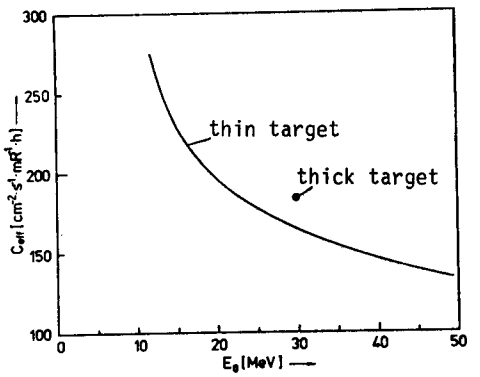

Fig. 5 Effective conversion factor for Bremsstrahlung

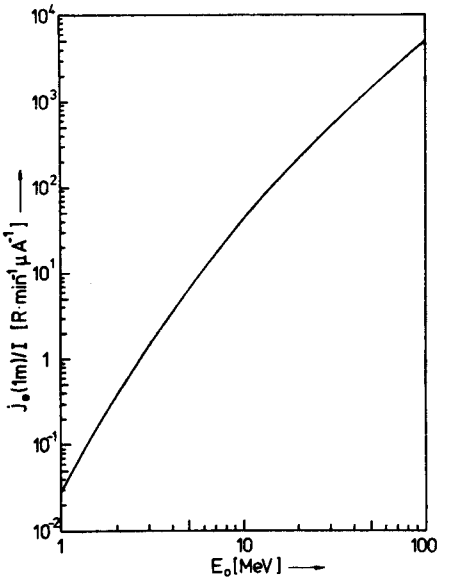

Fig. 6 X-ray emission rate from high-Z target of optimized thickness